Chassis Design and Analysis of an Autonomous Ground Vehicle (AGV) using Genetic Algorithm

Taher Deemyad
Department of Mechanical Engineering
Idaho State University
Pocatello, ID, USA
deemtahe@isu.edu

Ryan Moeller
Department of Mechanical Engineering Idaho State University
Pocatello, ID, USA
moelryan@isu.edu

Anish Sebastian
Department of Mechanical Engineering
Idaho State University
Pocatello, ID USA
sebaanis@isu.edu

***Abstract*- This paper analyzes the design of a prototype chassis for an autonomous ground vehicle (AGV). This prototype is a four-wheel powered vehicle which would be used for identifying and removal of potatoes affected by virus Y (PVY) in the field. Potato fields are fraught with rough terrain and deep irrigation ruts. Navigation of such a terrain is very challenging and demanding on the robot chassis. An optimization routine was used for finding the ideal size and material for the chassis. Seven different stress analysis were conducted to help narrow down the chassis design and material for the prototype. In addition to a general overview of the various vehicle sub-systems, a detailed description of the force and stress analysis for the chassis of this vehicle is provided. All stress analysis for this chassis passed the design requirements in CAD model (SolidWorks) and has been built and tested in the field.**

Keywords— Optimization, Stress Analysis, Force Analysis, Chassis, Autonomous Vehicle, Four Wheel Drive, CAD Stress Analysis

I. INTRODUCTION

To meet nutritional needs for the expanding human population by 2050, a projected 100-110% increase in crop production has been estimated, an increase, that is dependent on improvements in the efficiency of the current agro-ecosystem to minimize the continuation of our negative impact on global ecosystem [1]. The productivity of the agroecosystem has improved progressively in large owing to mechanization and automation of production systems [1]; however, as previously noted, global food demand is expected to double from 2005 levels by 2050. The results of this increased demand will push the agricultural industry and policy-makers to once again assess their decision-making and focus. This time the choice is between current practices and increasing land in agriculture, or moderate intensification coupled with new technologies. With each transition to incorporate new agricultural practices and technology, some in the agricultural sector choose to implement while others do not. Social and behavioral circumstances, along with a favorable policy environment, impact adoption rates of new technology and practices [2], [3]. Thus, in order to implement a co-robot system framework, it is imperative to understand the existing social, behavioral, and policy conditions and the possibility of making agricultural practice changes in the future. The concept of Integrated Pest Management (IPM) [4] was developed to reduce the negative impacts of reliance on intensive chemical use. Continuous monitoring of agricultural farms is a critical component of IPM practice. However, monitoring efficiency in large-scale farming is limited, as acknowledged by many producers. Precision agriculture [5] is a key component of the IPM strategy.

Achievements in computational, information, and robotic technologies can play a key role in reducing some of the costly agricultural inputs and in increasing yielding and sustainability. Steps for improved productivity and sustainability in the agroecosystem have been taken with IPM. A greater impact can be accomplished when used in conjunction with precision agriculture. However, its affordable and efficient implementation requires autonomous or collaborative robotics technology. This is the area in which this paper proposes to contribute. The research presented in this paper is a vital part of a larger, more complex problem. The broader scope of the project undertaken aims to answer the fundamental question of whether a multi-agent team comprised of humans, aerial and ground robots, and using multi-sensor fusion and learning techniques, could be the best solution for IPM and under what conditions. Currently, no such robotic system exists for agricultural applications. A part of this larger problem is the scalable co-robot which will be the autonomous ground vehicle (AGV) discussed in this paper.

A wide variety of potatoes are affected by the (potato virus Y) PVY virus and are also referred to as PVY carriers. Most of these varieties show mild or no symptoms when contaminated by the virus. Visual identification of the virus is especially difficult in the early stages [6]. Also, because of size of the fields and possibility of existence of viruses anywhere in the field, utilizing multi-robot exploration and task planning algorithm based on unknowingly distributed tasks can be useful [7], [8]. Virus detection methods including serological methods (ELISA) or molecular methods (PCR) are destructive, time-consuming, labor-intensive, and therefore very expensive. A non-destructive and fast method to detect viruses is the use of mid-wave infrared remote sensing [9].

PVY can be responsible for yield losses of up to 80% to 90% [9], [10]. Recent economic data indicates PVY reduces total potato production in Idaho by about 2.3 million hundred weight (cwt) annually. The direct cost of PVY to the Idaho economy is

about $19.5 million and economic modeling indicates the total impact exceeds $33 million annually [11]. Our previous research has shown that remote sensing techniques, coupled with machine learning algorithms, can differentiate virus-infected plants from non-infected neighbors based on electromagnetic energy absorbance and reflectance [12]. Hyperspectral cameras were used to achieve classification accuracies of 89.8%, compared to <50% when using only wavelengths detectable by the human eye. The algorithm used helps identify the infected crop at a very early stage in the crop growth cycle. This is very important, as later in the growth cycle aphids spread the PVY virus to healthy plants which result in significant crop loss. On detecting the infected plants, the standard procedure is to send a crew into the field to manually uproot the infected plants. Common disadvantages of this method are: a) Late Detection, as workers identify the infected plants visually, which is essentially further into their growing cycle, b) Time consuming: since this process is done manually; in an average field of a few acres to a few hundred acres it takes weeks or longer to complete the removal process. This allows additional time for the aphids to spread the virus, c) Additional cost on production, d) Significant loss of crops. These factors were the major motivating forces in the design and development of an autonomous ground vehicle (AGV) testbed to identify the infected plants early in the crop life-cycle. The AVG would be equipped with various sensors and an automatic roguing mechanism to dispose of the affected potatoes by PVY. The roguing mechanism will be selected between various mechanical designs preferably with a minimum number of actuators and smallest size [13], [14], [15] because the size and weight of the roguing mechanism will affect the final size and weight of AVG too. Also, soft robotic actuators [16] can be considered as one of the possible options in this mechanism.

II. AGV Workspace & Motion Study

A. Potato Field Simulation Information

The first step before designing the chassis and performing stress analysis is collecting all possible information about the environment in which this vehicle will be operated. This would give a better idea of the types of stresses the vehicle will be subjected to, and the type of analysis that needs to be done. In this research, after consulting with experts, local potato growers, visiting a potato field, and making accurate measurements, we created a simulated environment, which is shown in Fig. 1. This information was used to design the AGV chassis. As shown in Fig. 1, the height of each bump was 12 inches and the distance between two bumps was 24 inches.

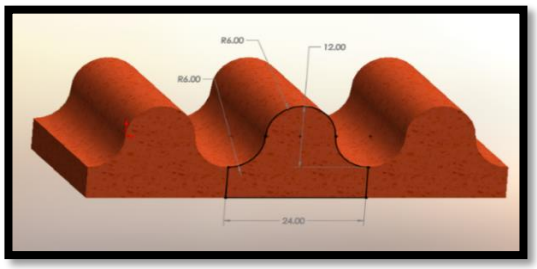

Fig. 1. Simulated shape and size of the terrain

B. Possible Stresses for a Four-Wheel Vehicle

In general, there are four main types of deformation for an automotive chassis [17].

1. Longitudinal Torsion:

If the force is applied in two opposite directions (up-down) on two opposite corners of the vehicle, a torsion load will affect the chassis. This load would cause a twist on the frame of the chassis.

2. Vertical Bending:

This force is made by the weight of all the various components of the vehicle like chassis, battery, motors, etc. plus all external loads like any moving parts on the vehicle, for example, a robotic arm. The reaction force would be acting on the axles in the upward direction.

3. Lateral Bending:

In this case, a lateral load causes a bending on the chassis because of sideways load along the length of the body of the vehicle. For instance, the force from the wind, road camber, or centrifugal forces.

4. Horizontal Lozenging:

This type of deformation happens when loads on two opposite sides of the vehicle are applied in opposite directions (forward-backward forces). These forces are made by the difference in the height of the roadway or the reaction force from the road over the vehicle going forward.

However, according to the shape of the potato field and different possible paths in which this vehicle is supposed to drive Fig. 2, maximum force affecting the chassis is the vertical load made by its weight. So, among all the deformations mentioned in II B, the focus of this research is on the vertical bending and torsion stresses caused by the weight of the vehicle.

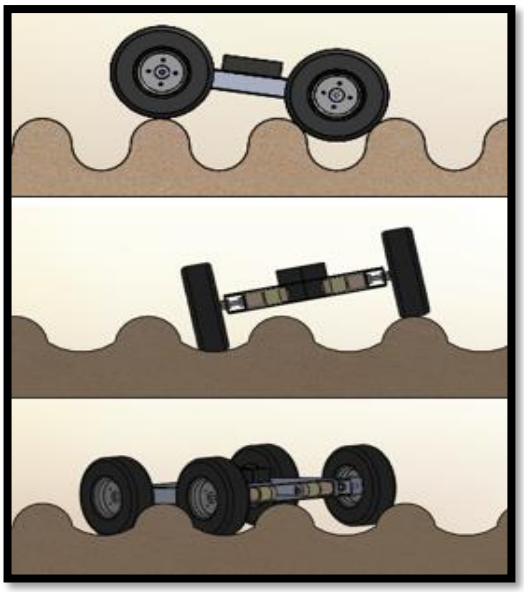

Fig. 2. Simulated Terrains Encountered in Field

III. Parts of Vehicle & Specification

A. Parts of vehicle & specification

As shown in Fig. 3, this vehicle contains 10 components. Each wheel is independently actuated with individual electric motors to maximize power and for better control of the vehicle. The chassis of this vehicle is made of three main pieces, bottom plate, top plate, and two motor mount tubes. Motor mount tubes are welded to the bottom plate, and the top of the tubes are bolted to the top plate. Based on the tasks and ruggedness of the field, four 10-inch pneumatic wheels with aggressive treads were selected for this vehicle. The quantity and weight of each of the components are provided in Table. I.

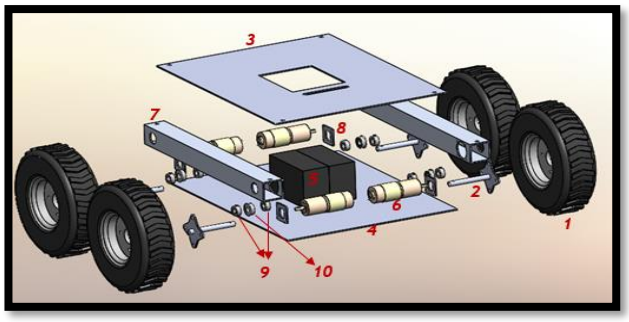

Fig. 3. AGV components

TABLE I: NAME, QUANTITY, AND WEIGHT OF EACH PART

#	Part	QTY	Wt kg-(lb)
1	Wheel	4	14.97-(33)
2	Shaft	4	0.454-(1)
3	Top Plate	1	1.36-(3)
4	Bottom Plate	1	1.36-(3)
5	Battery	2	2.27-(5)
6	Motor	4	0.91-(2)
7	Motor Mount Tube	2	1.36-(3)
8	Motor Mount Plate	4	0.454-(1)
9	Clamp Collars	8	0.23-(0.5)
1o	Steel Ball Bearing Flanged	4	0.23-(0.5)

B. Material selection & Size of the chassis

Except for the chassis which was designed, analyzed, and built for this project, the other components were selected and ordered from different vendors to satisfy the overall design requirements. To find the appropriate material for the chassis, between Aluminum Alloy 6061, Steel ASTM A36, and Steel AISI 4130, Aluminum alloy 6061 was selected because of higher stiffness and lower weight. Relevant material properties are presented in Table. II. The size of the bottom and top plates are $53.3cm \times 43.2cm \times 0.3175cm$ ($21in \times 17in \times 0.125in$) and Motor Mount tube has a thickness of $0.3175cm$ ($0.125in$).

TABLE II:SPECIFICATION OF ALUMINUM ALLOY 6061

Properties	Value
Yield Strength	55.15 MPa
Tensile Strength	124 MPa
Elastic Modulus	69000 MPa
Poisson's Ratio	0.33
Mass Density	2700 kg/m3
Shear Modulus	26000 MPa

IV. Results & Discussion

We selected a rectangular modular shape for the AGV chassis to accommodate all the components and to allow for future modifications. On mounting all the components, the maximum possible load was applied to the chassis. In this section, material selection for the chassis and the best overall size and weight are discussed. These were calculated based on an optimization algorithm. Thereafter, force analysis of the chassis will be discussed. Finally, seven stress analysis tests are provided to ascertain that this vehicle will not fail in its intended operating environment.

A. Chassis Optimization

Genetic Algorithm was utilized to optimize the overall shape, minimize the weight without compromising the structural integrity of the AGV. The overall weight of the vehicle, and the terrain to be navigated and the onboard instrumentation are the critical factors that dictate the required power from actuators and the capacity of batteries which could be used. We do not have control over the weight of the onboard instrumentation or the battery pack. Therefore, we targeted the weight of the chassis. This was the objective function considered for optimization. Additionally, there were several equality and non-equality constraints on this optimization. For instance, the minimum thickness for metal plates available at the local hardware store is 0.003m, or the maximum stress over chassis (multiplied by the factor of safety) must be less than the yield strength of the specified material, which was considered in constraints. The maximum stress over chassis will be found from equation (1).

$$\sigma_{bend-max} = \frac{M \times c}{I} \qquad (1)$$

M = the internal bending moment

c = the perpendicular distance from the neutral axis to the farthest point on the section

I = the moment of inertia of the section area about the neutral axis

This optimization was repeated for three different materials and a minimum total weight of chassis for each of them was found. Symbols for different parts of chassis were shown in Fig. 4. The size of each of the components after optimization is provided in Table. III. The optimum size (as was expected) is similar for all three materials. Aluminum Alloy 6061 has minimum weight as compared to others. So, it was selected for the chassis. Because of the availability and size of the other parts of the vehicle, some of the dimensions for chassis in the final design were a little different from this table (but very close to the calculated value).

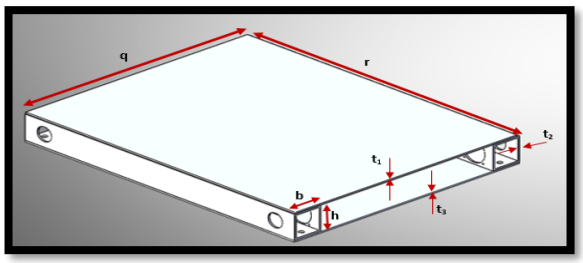

Fig. 4. Chassis

TABLE III: OPTIMIZATION RESULTS FOR THREE DIFFERENT MATERIALS FOR CHASSIS

Parameters	Aluminum Alloy 6061	Steel ASTM A36	Steel AISI 4130
t1 (m)	0.003	0.003	0.003
t2 (m)	0.003	0.003	0.003
t3 (m)	0.003	0.003	0.003
b (m)	0.05	0.05	0.05
h (m)	0.05	0.05	0.05
q (m)	0.4	0.4	0.4
r (m)	0.5	0.5	0.5
W (kg)	4.7628	13.8474	13.8474

B. Force Analysis

The total weight of the vehicle including all components is 23.5868 kg (52 lbs). This weight makes a total force of 231.386 N which causes a vertical load of 57.847 N over each wheel of this vehicle. However, for all stress analysis tests in this research, a factor of safety (F.S.) of 4 was chosen. Therefore, after importing the F.S. on the calculation, the final force over each wheel will be 231.386 N.

C. Stress Analysis

Seven different stress analyses have been described in this section. For all stress analyses, a solid mesh with a size of 0.0051m (0.2in) and a maximum aspect ratio of 13.933 was used. More information about the mesh mentioned in Table. IV.

TABLE IV: MESH INFORMATION

Total Nodes	79959
Total Elements	41264
Element Size	0.831685 in
Tolerance	0.0415842 in
% of elements with Aspect Ratio < 3	66.4
% of elements with Aspect Ratio > 10	0.172

Test 1: Bending stress #1

This bending stress analysis is for a scenario when three wheels of the vehicle are at a lower level than the fourth one (Fig. 5). In this case, three connection links for the wheels will be assumed fixed (triangles in Figure 5) and a vertical load will be concentrated on the fourth wheel (upward arrow).

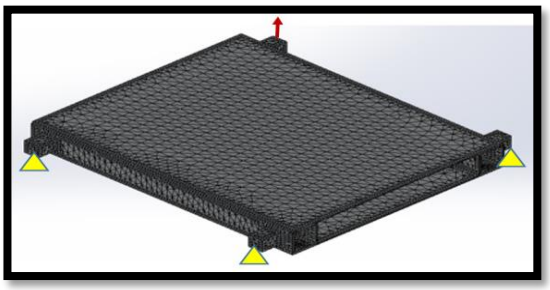

Fig. 5. Reaction forces in test 1

Test 2: Bending stress #2

In this case, two wheels on the left are at a lower level than the wheels on the right. Therefore, the weight of the vehicle causes bending stress on the chassis In Fig. 6, two connection links for left wheels are assumed fixed (triangles in Figure 6) and load distributed between connections links of right wheels are in the same direction (both reaction forces are in the upward direction denoted by the arrows pointing up).

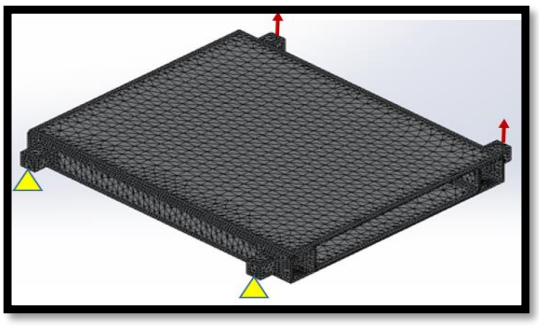

Fig. 6. Reaction forces in test 2

Test 3: Bending stress #3

In this case, two wheels in front of the vehicle are at a lower level than the wheels on the rear of the AGV. So, it would be similar to the second test and the weight of the vehicle causes bending stress on the chassis but this time two connection links for the front wheels are fixed and loaded in the same direction (both reactions forces upward direction) distributed between connection links of rear wheels (Fig. 7)

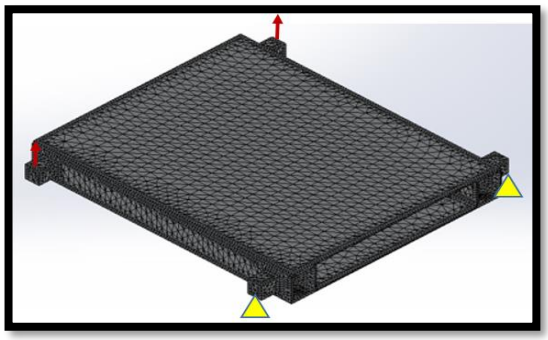

Fig. 7. Reaction forces in test 3

Test 4: Bending stress #4

This analysis loads the chassis when two diagonally opposite wheels are at a higher elevation than the other two wheels. Fig. 8 shows this situation when two connection links of two diagonally opposite wheels are fixed and two others are affected by the upward load which makes a bending on the chassis.

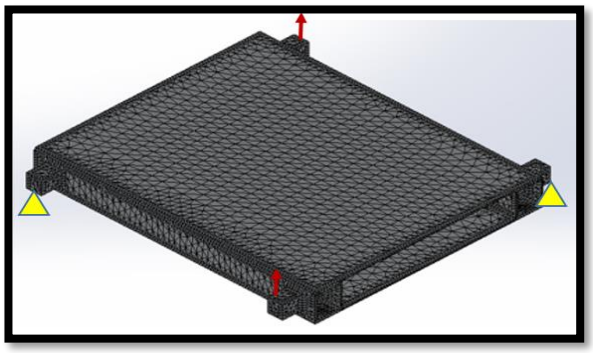

Fig. 8. Reaction forces in test 4

Test 5: Torsion stress #1

This test is similar to the second test with the only change in the way the load is affecting the connection links for the right wheels. As it is shown in Fig. 9, one of the loads is going up when the other one is going down which causes torsional stress rather than bending over the chassis.

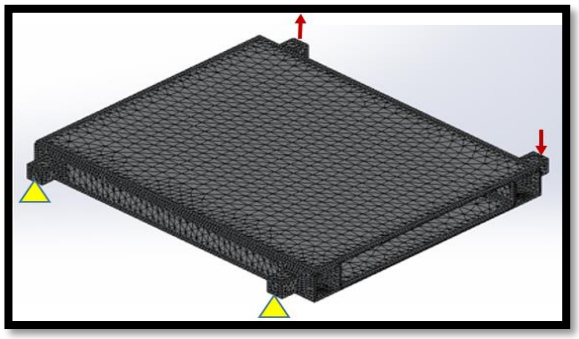

Fig. 9. Reaction forces in test 5

Test 6: Torsion stress #2

This test is also the same as the third test, but the load is acting opposite to each other. One of the loads on the back is going up when the other one is pointing down which causes twist on the chassis and makes torsional stress rather than bending over the chassis (Fig. 10).

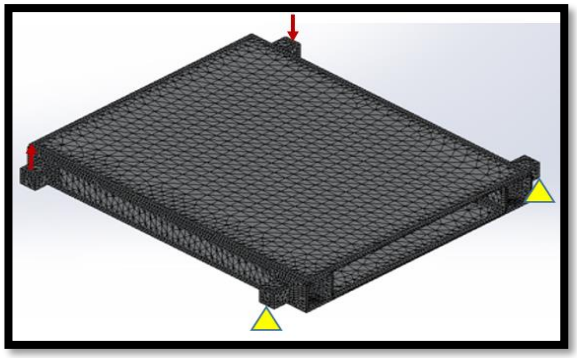

Fig. 10. Reaction forces in test 6

Test 7: Torsion stress #3

The last test is torsional too. Fixed links and the position of the load are the same as the fourth test with only difference in the direction of load. From Fig. 11, one of the loads is going up when the other one is going down which causes torsional stress.

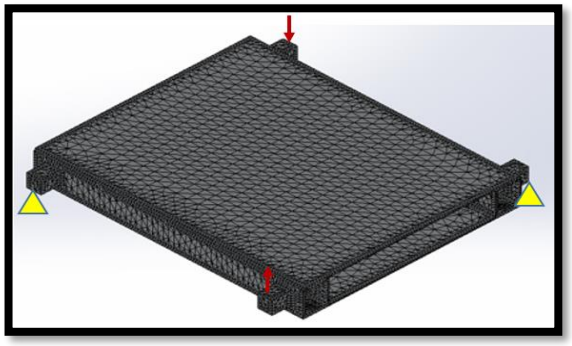

Fig. 11. Reaction forces in test 7

The final results for all seven stress analysis are presented in Table. V. The maximum stress and displacement occurred in test 2 when two wheels in the left and two wheels in the right are not at the same level, and this caused bending stress over the chassis. However, maximum strain occurred in the third test when the front and back wheels were not at the same level. This also made bending stress on the chassis.

TABLE V: FINAL RESULTS FOR STRESS, DISPLACEMENT, AND STRAIN OF ALL 7 TESTS

Test	Stress (N/m^2)	Strain	Displacement (m)
1	2.826e+7	2.469e-4	2.170e-4
2	5.065e+7	4.136e-4	6.013 e-3
3	4.514e+7	4.783e-4	3.707e-4
4	2.181e+7	1.972e-4	1.619e-4
5	2.185e+7	1.596e-4	3.369e-4
6	2.185e+7	2.263e-4	1.579e-4
7	3.703e+7	3.933e-4	3.653e-4

Displacement and stress for test 2, respectively are showed in Fig. 12 & Fig. 13 Also, strain for test 3 is presented in Fig. 14.

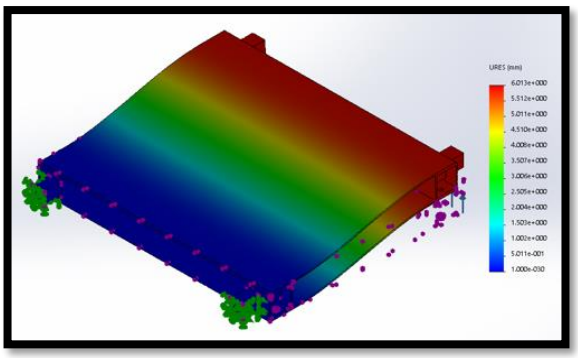

Fig. 12. Displacement in test 2

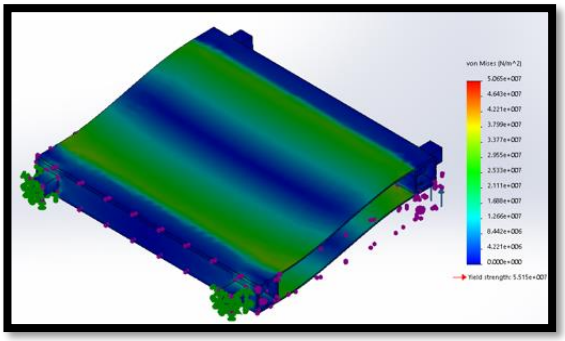

Fig. 13. Stress in test 2

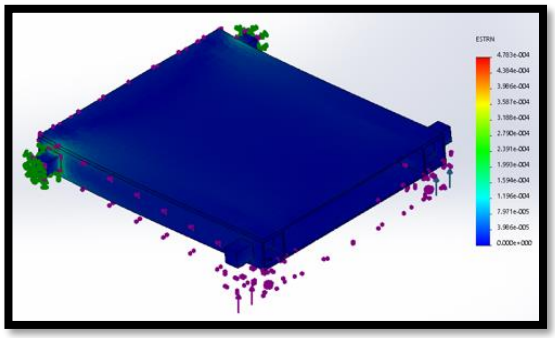

Fig. 14. Strain in test 3

The stresses on the chassis in comparison to the maximum stress and yield strength of aluminum alloy 6061, shows that the designed chassis wouldn't fail for any simulated condition in the field. This chassis has been built and has been tested in the field and has performed as per expectations. There is sufficient space on top of the chassis for all electronic equipment like a GPS, micro-controller and in the future a robotic arm platform. Fig. 15 shows the actual built to specification prototype.

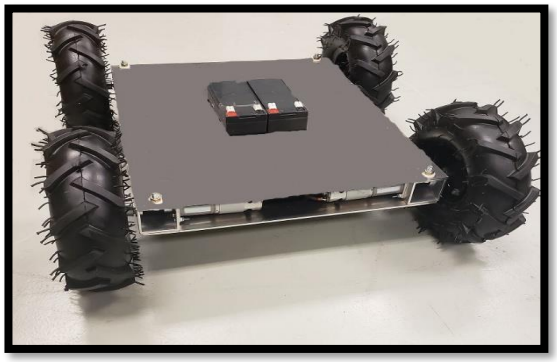

Fig. 15. Autonomous ground vehicle

V. Conclusion

In this paper, the process of chassis design for an autonomous ground robot for agriculture was discussed. First, using the Genetic Algorithm, we calculated the optimum size of the chassis and selected the best material for the application while minimizing weight. Next, we performed the force analysis of the chassis. Finally, based on possible stress on the chassis, we did seven stress analysis tests in SolidWorks, 4 bending tests, and 3 torsion tests. The maximum stress and displacement occur when two wheels in the left are assumed fixed and force was applied to the two right wheels. However, final results show this chassis is very capable and can withstand all the possible simulated stresses. The autonomous vehicle with the above-decribed chassis was fully assembled and successfully was tested in a field.

References

[1] D. Tilman, C. Balzer, J. Hill, and B.L. Befort, 2011. Global food demand and the sustainable intensification of agriculture. Proceedings of the national academy of sciences, 108(50), pp.20260-20264.

[2] J.L. Araus, and J.E. Cairns, 2014. Field high-throughput phenotyping: the new crop breeding frontier. Trends in plant science, 19(1), pp.52-61.

[3] J.M. McGuire, L.W. Morton, J.G. Arbuckle Jr, and A.D. Cast, 2015. Farmer identities and responses to the social–biophysical environment. Journal of Rural Studies, 39, pp.145-155.

[4] L.E. Ehler, 2006. Integrated pest management (IPM): definition, historical development and implementation, and the other IPM. Pest management science, 62(9), pp.787-789.

[5] S. Haneklaus, H. Lilienthal, and E. Schnug, 2016, July. 25 years precision agriculture in germany–a retrospective. In 13th International Conference on Precision Agriculture.

[6] P. Nolte, J.M. Alvarez, and J.L. Whitworth, 2009. Potato virus Y management for the seed potato producer. University of Idaho Extension CIS1165.

[7] M. Dadvar, S. Moazami, H. R. Myler, and H. Zargarzadeh, "Multiagent task allocation in complementary teams: a hunter-and-gatherer approach," Complexity, vol. 2020, Article ID 1752571, 15 pages.

[8] M. Dadvar, S. Moazami, H. R. Myler, and H. Zargarzadeh, "Exploration and coordination of complementary multi-robot teams in a hunter and gatherer scenario," 2019, https://arxiv.org/abs/1912.07521.

[9] M. C. Mayer, "Early detection of virus infections in potato by aphids and infrared remote sensing", MS Thesis, Department of Crop Production Ecology, Swedish Univ. of Agricultural Sciences, 2016.

[10] A.V. Karasev, and S.M. Gray, 2013. Continuous and emerging challenges of Potato virus Y in potato. Annual Review of Phytopathology, 51, pp.571-586.

[11] W. Buhrig, M.K. Thornton, N. Olsen, D. Morishita, and C. McIntosh, 2015. The influence of ethephon application timing and rate on plant growth, yield, tuber size distribution and skin color of red LaSoda potatoes. American journal of potato research, 92(1), pp.100-108.

[12] L.M. Griffel, D. Delparte, and J. Edwards, 2018. Using Support Vector Machines classification to differentiate spectral signatures of potato plants infected with Potato Virus Y. Computers and electronics in agriculture, 153, pp.318-324.

[13] T. Deemyad, N. Hassanzadeh, and A. Perez-Gracia. Coupling mechanisms for multi-fingered robotic hands with skew axes. In Mechanism Design for Robotics (MEDER). Springer, 2018.

[14] T. Deemyad, O. Heidari, and A. Perez-Gracia. Singularity Design for RRSS Mechanisms. In USCToMM Symposium on Mechanical Systems and Robotics (MSR) Conferences. Springer, 2020.

[15] T. Deemyad. Design of Five-fingered Underactuated Hand for Two-position Tasks (Master's Thesis, Idaho State University), 2016.

[16] S. Habibian. "Analysis and Control of Fiber-Reinforced Elastomeric Enclosures (FREEs)." (Master's Thesis. 229, Bucknell University), 2019.

[17] W.B. Riley and A.R. George, 2002. Design, analysis and testing of a formula SAE car chassis (No. 2002-01-3300). SAE Technical Paper.